

Bulk Viscosity Sensing

Hannes Antlinger¹, Roman Beigelbeck², Stefan Clara¹, Thomas Voglhuber-Brunnmaier^{1, 2}, Samir Cerimovic³, Franz Keplinger³, Bernhard Jakoby¹

¹ *Institute for Microelectronics and Microsensors, Johannes Kepler University Linz, Austria,*

² *Zentrum für Integrierte Sensorsysteme, Danube University Krems, Austria*

³ *Institute of Sensor and Actuator Systems, TU Wien, Austria
bernhard.jakoby@jku.at*

Abstract:

The second coefficient of viscosity (or bulk viscosity) is a parameter that, just as the shear viscosity, is suitable, e.g., for condition monitoring applications. Its measurement is based on the attenuation of bulk acoustic waves in the analyte and is thus based on measurements in the bulk of a liquid rather than a surface layer (as in many shear viscosity sensors). In our contribution, we review the relevant considerations associated with this approach including spurious diffraction and reflections.

Key words: bulk viscosity, liquid condition monitoring, physical fluid properties, diffraction, pressure waves.

Introduction

Sensing physical liquid properties is of utmost importance in many technical processes, especially modern process control shows an increasing demand for sensors determining physical fluid parameters. Examples for parameters to be determined are mass density, sound velocity, (shear-) viscosity and thermal conductivity. The sensors should ideally be low cost, robust against environmental influences like e.g., vibrations or temperature, small in size and weight and preferable suited for online condition monitoring. Furthermore they should be qualified for mass production and enable a maintenance free operation over lifetime. Standard laboratory equipment used to perform this task is often expensive, service intensive, bulky and in many cases requires manual sample withdrawal. Due to the mentioned issues the latter is often less suited for online condition monitoring applications. Recently a lot of effort has been spent on miniaturized viscosity sensors [1]. The latter often sense the so called shear-viscosity in combination with other liquid parameters, like e.g., sound velocity, mass density or the characteristic acoustic impedance [1], [2], [3]. Sensor principles utilizing the excitation of shear waves (e.g. TSM resonators operating in the MHz regime or small vibrating structures operated in the kHz regime) into the liquid to be investigated suffer from two serious drawbacks. First, they typically only feature a small penetration depth of shear waves into the liquid

so that they are prone to surface contamination and their application for sensing emulsions featuring a particle size in the range of the penetration depth of the excited shear waves (e.g., a few microns, depending on the excitation frequency and the shear viscosities to be investigated) or even greater is limited. Second, the generation of shear waves also generates scarcely damped compressional waves which could lead to spurious interferences when they are reflected by nearby objects [4]. Beside the well established shear viscosity, the bulk- or so called second coefficient of viscosity has been considered as promising candidate for online condition monitoring applications. Sensors for the second coefficient of viscosity utilize acoustic pressure waves. Therefore the bulk of the sample is being sensed rather than only a thin fluid layer. The fluid induced damping of the excited acoustic pressure waves gives a measure for the so called acoustic viscosity [5]. As shown in [5], the acoustic viscosity represents a combination of the shear and bulk viscosity. In this contribution we present the basic sensor setup as well as an according modeling and strategy to determine the bulk viscosity of a liquid under investigation.

Theory and basic sensor setup

As described above the proposed approach is based on determining the damping of acoustic pressure waves in a liquid. Fig. 1 [6] depicts the basic sensor setup. Two planar rigid boundaries separated by a distance h form a sample chamber which encloses to liquid to be

monitored. One boundary carries a flush mounted PZT transmitter (diameter d_T and thickness l_T) exciting acoustic pressure waves while the opposite boundary carries a PZT receiver (diameter d_R and thickness l_R) receiving the attenuated acoustic waves.

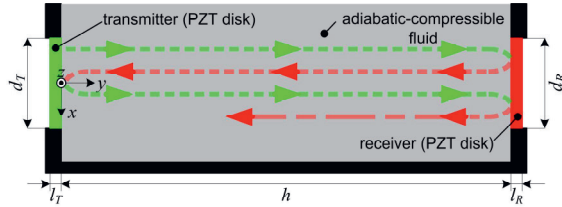


Fig. 1. Basic sensor setup.

The transmitting, as well as the receiving device are operated in the so called “33-mode” also called thickness-extensional mode. The mounting of the transducer devices ensures that the outer faces (the ones not being in contact with the liquid) of both transducers are facing air yielding in a defined, yet low acoustic impedance which results in a well defined termination impedance of the transducers outer acoustic ports. Due to the mismatch in acoustic impedances of the PZT transducers inner faces and the liquid in the sample chamber multiple reflections of excited acoustic pressure waves can occur. From the theory of acoustic wave propagation the behavior of pressure waves in liquids is well known [5]. As described in [7] for the viscous damping both the shear viscosity η as well as the bulk viscosity η_B need to be considered. Within literature the definition of these two coefficients is non uniform. For our work we adopted the notation from [7] where the linearized Navier-Stokes equation appears as,

$$\rho_{fl} \ddot{\mathbf{u}} = \frac{1}{\zeta_s} \nabla (\nabla \cdot \mathbf{u}) + \left(\frac{\eta}{3} + \eta_B \right) \nabla (\nabla \cdot \dot{\mathbf{u}}) + \eta \nabla^2 \dot{\mathbf{u}}. \quad (1)$$

In (1) \mathbf{u} is the displacement vector, ρ_{fl} denotes the mass density and ζ_s represents the adiabatic compressibility. The dots denote derivation with respect to time.

1D-Sensor model

In this section we describe the derivation of a simple 1D-model for the sensor setup introduced above. As described in detail in [8] each PZT disk transducer can be modeled as a three port network with two acoustic ports and one electric port as depicted in Fig. 2.

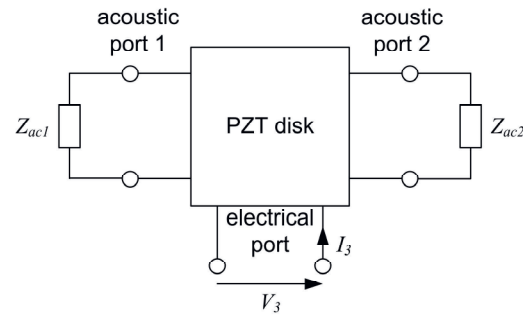


Fig. 2. Three-port PZT transducer model.

Z_{ac1} and Z_{ac2} are the acoustic load impedances. In the frequency domain, the electric impedance Z_3 of the PZT transducer loaded with the acoustic impedances Z_{ac1} and Z_{ac2} can be derived as [8], [9],

$$Z_3 = \frac{V_3}{I_3} = \frac{1}{j\omega C_0} \left[1 + \frac{k_T^2}{\bar{\beta}_a l} \cdot \frac{j(Z_{ac1} + Z_{ac2})Z_C \sin(\bar{\beta}_a l) - 2Z_C^2 [1 - \cos(\bar{\beta}_a l)]}{(Z_C^2 + Z_{ac1}Z_{ac2})\sin(\bar{\beta}_a l) - j(Z_{ac1} + Z_{ac2})Z_C \cos(\bar{\beta}_a l)} \right],$$

$$C_0 = \frac{\epsilon^s A}{l}, Z_C = A\sqrt{\rho_{PZT} c^D}, \bar{\beta}_a = \omega \sqrt{\frac{\rho_{PZT}}{c^D}}. \quad (2)$$

In (2) C_0 denotes the clamped transducer capacitance, Z_C represents the acoustic impedance of the transducer with the active acoustic area A , $\bar{\beta}_a$ is the effective wavenumber of longitudinal waves within the PZT ceramic and ω is the angular frequency. ρ_{PZT} (mass density), ϵ_s (permittivity for constant strain) and k_T (electromechanical coupling) are the PZT material parameters for the “33” (longitudinal) operation mode of the piezoceramic, which can be obtained from the PZT material datasheet [10]. Due to the low characteristic acoustic impedance of air, for the acoustic ports facing air backing, the acoustic load impedances $Z_{ac,i}$ can be approximately considered as an acoustic shortcut. In analogy to an electric transmission line the fluid in the sample chamber is modeled by an acoustic transmission line with the length h , a characteristic acoustic impedance z_{fl} and a propagation constant γ_{fl} . The frequency domain values for z_{fl} and γ_{fl} can be obtained as [8],

$$z_{fl} = \sqrt{\rho_{fl} \left[\rho_{fl} c_{fl}^2 + j\omega \left(\frac{4}{3} \eta + \eta_B \right) \right]}, \quad (3)$$

$$\gamma_{fl} = j\omega \sqrt{\frac{\rho_{fl}}{\rho_{fl} c_{fl}^2 + j\omega \left(\frac{4}{3} \eta + \eta_B \right)}}. \quad (4)$$

From (3) and (4) it can be seen that the following fluid parameters determine the fluid transmission line parameters: sound velocity c_{fl} , mass density ρ_{fl} , shear viscosity η and bulk viscosity η_B . ω is the angular frequency of the excitation signal. We note that the presented sensor setup is suited for the determination of $(\frac{4}{3}\eta + \eta_B)$. Therefore to determine the bulk viscosity η_B the shear viscosity η has to be firmly established, e.g. by utilizing a shear viscosity sensor. The 1D-model for the full sensor setup is shown in Fig. 3. An electric signal source provides the electric input signal V_{IN} which is converted into an acoustic output signal by the transmitter. The receiver converts the received (acoustic) input signal to an electrical output signal V_{OUT} . The electric port of the receiver is loaded with the load impedance Z_L e.g. the input impedance of an oscilloscope.

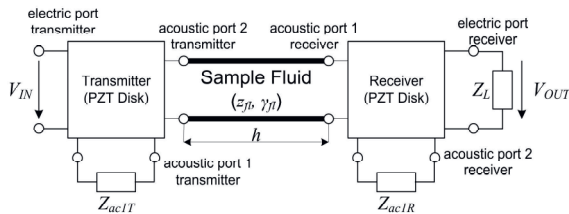


Fig. 3. 1D-sensor model.

From theory it is known, that the frequency domain viscous damping coefficient α of a liquid in dB can be obtained as [11],

$$\alpha = 4.343h \left[\frac{\omega^2}{\rho_{fl} c_{fl}^3} \left(\frac{4}{3}\eta + \eta_B \right) \right]. \quad (5)$$

Utilizing sine wave burst signals enables the combination of approaches suitable for continuous wave operation as well as for transient operation. Selecting a burst length so that transient settling is achieved within the duration of the burst but at the same time superposition of multiple reflection signals is avoided enables the use of damping coefficients obtained from frequency domain considerations. Thus the total measured attenuation α_{MEAS} can be determined from the settled voltage amplitudes as,

$$\alpha_{MEAS} = 20 \log \left(\frac{V_{IN}}{V_{OUT}} \right). \quad (6)$$

Beside the viscous attenuation several other loss mechanisms take effect and therefore contribute to α_{MEAS} . The individual loss mechanism will be discussed below. The transmitter as well as the receiver can be described by an electroacoustic / acoustoelectric conversion gain. This conversion gain includes losses due to the

mismatch of the acoustic impedances of the PZT transducers and the liquid in the sample chamber and losses due to the mounting of the transducers. Furthermore additional losses due to spurious diffraction losses along the sample chamber propagation path of the acoustic waves have to be considered. Especially for low viscous fluids diffractions losses can become the dominant loss mechanism compared to the viscous attenuation losses. Thus as can be seen in detail in [12], [13], [14] diffraction losses can become an important source of error to be considered in correction procedures. An in depth discussion including the derivation of a method for calculating theoretical values for the diffraction losses is presented in [15]. Considering the discussed conversion gain α_C and diffraction losses α_D , α can be obtained from the measured attenuation as,

$$\alpha = \alpha_{MEAS} - \alpha_D - \alpha_C. \quad (7)$$

Combining (5) and (7) results in a solution for the bulk viscosity η_B as,

$$\eta_B = \frac{\rho_{fl} c_{fl}^3}{\omega^2} \left(\frac{\alpha_{MEAS} - \alpha_D - \alpha_C}{4.343h} \right) - \frac{4}{3}\eta. \quad (8)$$

The determination of α_D and α_C based on a simple calibration procedure will be presented in the measurement results section.

Prototype Device

A first demonstrator device which has been built to obtain experimental results is depicted in Fig. 4 [6].

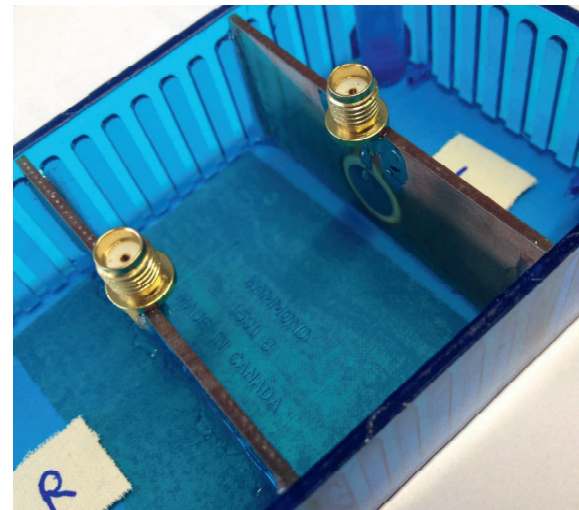


Fig. 4 First prototype device.

For this device the distance h according to Fig. 3 is 24 mm. A standard plastic case was used as main body while the both orthogonal rigid boundaries with the flush mounted PZT transducers are constructed from 1.5 mm copper coated FR4 PCB material. Each PCB

side has a 35 μm thick copper coating. Both transducers have been chosen to be equal. PI-ceramic PIC255 PZT disks [10] with an active electrode diameter of $d_R = d_T = 9\text{ mm}$ and an thickness $l_T = l_R = 0.5\text{ mm}$ have been utilized. Two SMA connectors provide the electric connection to an excitation signal source or an oscilloscope.

Measurement Results

For the following measurements, an 81150A signal generator from Agilent was used to excite the PZT transmitter. A 50 cycle sine burst signal with a frequency of 4.2859 MHz was utilized as drive signal. The transmitter as well as the receiver voltages have been recorded with a LeCroy Waverunner 44Xi oscilloscope. To determine the conversion gain α_C a reference measurement with a known test fluid (distilled water at a temperature of 25 °C) has been performed. For the settled amplitudes of the transient input and output voltages a total measured attenuation α_{MEAS} of 9.9 dB has been determined. Using (5) and the procedure described in [15] with the material data given in [16] results in theoretical values for the viscous attenuation $\alpha = 0.086\text{ dB}$ and $\alpha_D = 1.23\text{ dB}$ for the diffractions losses. Considering the obtained theoretical loss values results in a conversion gain for this setup, at the used excitation frequency, of $\alpha_C = 8.584\text{ dB}$. For the further presented measurement results the diffraction losses as well as the conversion gain (including the mismatch in acoustic impedances) are assumed to be constant as the determining values for the unknown liquid are supposed to only differ by a small value resulting in a first order negligible error. A more accurate correction procedure will be part of further research. In a next step the sample chamber was filled with S200 viscosity standard oil at different temperatures T .

Tab. 1: S200 material data

$T / ^\circ\text{C}$	$c_f / \text{m/s}$	$\rho_f / \text{kg/m}^3$	$\eta / \text{mPa}\cdot\text{s}$
20	1497.96	886.83	602.20
25	1478.97	883.75	418.10
40	1425.09	874.57	160.50
50	1391.15	868.45	93.25

Table 1 shows the S200 material data for the different temperature values. The shear viscosity values have been given by the material datasheet while the sound velocity c_f as well as the mass density ρ_f have been measured using an Anton-Paar DSA5000 density and sound velocity meter. Table 2

shows the obtained measurement results for the total signal attenuation α_{MEAS} , the values for α_D and α_C obtained from the calibration procedure and the determined bulk viscosity values η_B . Fig. 5 depicts the S200 viscosity standard oil datasheet values for the shear viscosity as well as the determined bulk viscosity. As expected with increasing temperature and decreasing shear viscosity also the bulk viscosity decreases. We note that no nominal bulk viscosity data for the S200 viscosity standard is available. As an indication literature [17] provides a typical ratio (η_B / η) of 1 with a range of rarely greater than 20 or less than 0.1. As shown in Fig. 6 for our measurements we determined values in the range of 0.42 ... 1 which indicates that our measurements meet this requirement. Nevertheless for precise absolute value measurements the sensor as well as the underlying model and calibration procedures need to be refined. As well as firmly established reference data is needed.

Tab. 2: Measured attenuation, correction values and obtained bulk viscosity values for different temperatures.

$T / ^\circ\text{C}$	$\alpha_{MEAS} / \text{dB}$	$\alpha_D + \alpha_C / \text{dB}$	$\eta_B / \text{mPa}\cdot\text{s}$
20	36.7	9.814	257.35
25	30.3	9.814	217.39
40	20.4	9.814	140.49
50	17.0	9.814	97.95

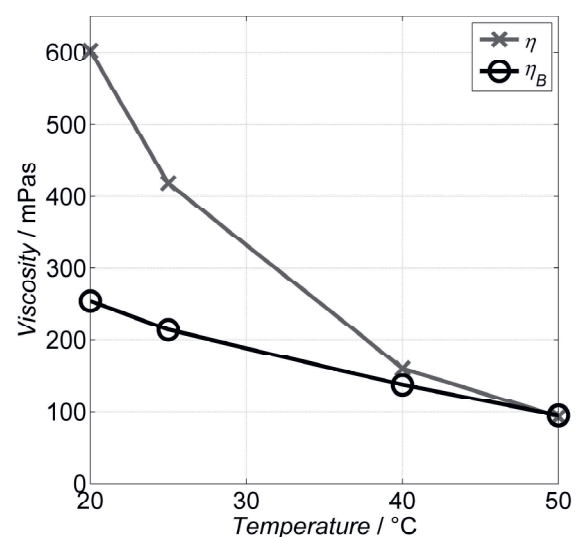


Fig. 5: Shear viscosity (datasheet values) and determined bulk viscosity values (measurement) over temperature.

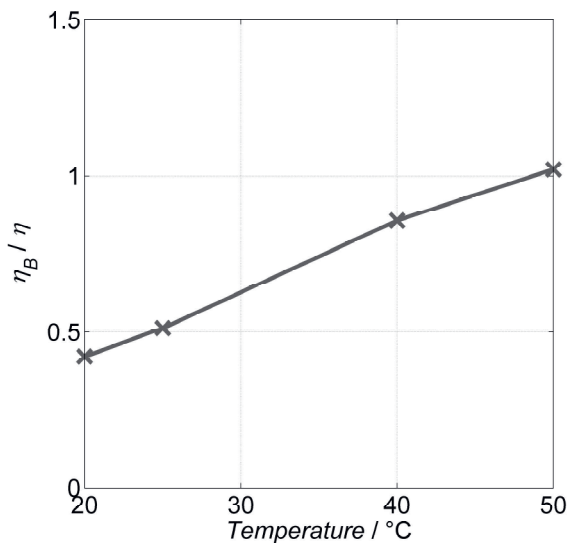


Fig. 6. Determined bulk viscosity to shear viscosity ratio over temperature.

Summary and Outlook

We presented the feasibility of a sensor concept allowing the determination of the bulk viscosity or second coefficient of viscosity. The basic sensor setup as well as a simple 1D frequency domain model have been derived. Measurement data obtained with a first experimental device confirmed the expected behaviour. Future research will include refinements in the calibration procedures as well as further verification of the obtained data and improved prototype devices.

References

- [1] B. Jakoby et al, "Miniaturized Sensors for the Viscosity and Density of Liquids-Performance and Issues", IEEE Trans. on Ultrason., Ferroelec., and Freq. Contr., vol. 57, no. 1, pp. 111–120, 2010.
- [2] H. Antlinger et al., Sensing the characteristic acoustic impedance of a fluid utilizing acoustic pressure waves, Sensors and Actuators A: Physical, ISSN 0924-4013 4247, <http://dx.doi.org/10.1016/j.sna.2012.02.050>.
- [3] Jakoby, B.; Vellekoop, M.J.; , "Physical Sensors for Liquid Properties," Sensors Journal, IEEE , vol.11, no.12, p.3076-3085, Dec. 2011.
- [4] T. Voglhuber-Brunnmaier, B. Jakoby, Efficient spectral domain formulation of loading effects in acoustic sensors, Sensors and Actuators A: Physical, Available online 8 January 2012, ISSN 0924-4247, 10.1016/j.sna.2011.12.052. (<http://www.sciencedirect.com/science/article/pii/S0924424712000040>).
- [5] L.D. Landau, E.M. Lifshitz, Fluid Mechanics, Second Edition, Butterworth-Heinemann, 1987.
- [6] H. Antlinger, R. Beigelbeck, S. Clara, S. Cerimovic, F. Keplinger and B. Jakoby, "Investigation and Modeling of an Acoustoelectric Sensor Setup for the Determination of the Longitudinal Viscosity," in IEEE Transactions on Ultrasonics, Ferroelectrics, and Frequency Control, vol. 63, no. 12, pp. 2187-2197, Dec. 2016. doi: 10.1109/TUFFC.2016.2611563
- [7] Frank M. White, Viscous Fluid Flow, Third Edition, McGraw-Hill International Edition, 2006.
- [8] Arnau Vives, Antonio (Ed.), Piezoelectric Transducers and Applications, Springer Verlag, 2nd ed., 2008.
- [9] Kino, Gordon S., Acoustic waves: devices, imaging, and analog signal processing, Prentice-Hall, Inc. 1987.
- [10] PI-Ceramic, PIC255 material coefficients data, <http://www.piceramic.com>.
- [11] H. S. Ju, E. Gottlieb, D. Augenstein, G. Brown, B. R. Tittmann, "An empirical method to estimate the viscosity of mineral oil by means of ultrasonic attenuation," Transactions on Ultrasonics, Ferroelectrics, and Frequency Control, 57(7) pp. 1612-1620, 2010.
- [12] H. Seki et al, Diffraction effects in the Ultrasonic Field of a Piston Source and Their Importance in the Accurate Measurement of Attenuation, J. Acoust. Soc. Am. 28 230-8, 1956.
- [13] Leveque, G., Rosenkrantz, E., Laux, D.: Correction of diffraction effects in sound velocity and absorption measurements. Measurement Science & Technology 18(11), 3458–3462 (2007).
- [14] Aouzale, N.; Chitnalah, A.; Jakjoud, H.; Kourtiche, D., "PSPICE Modelling Diffraction Effects in Pulse Echo Ultrasonic System, "Electronics, Circuits and Systems, 2007. ICECS 2007. 14th IEEE International Conference on , vol., no., pp.54,57, 11-14 Dec. 2007 doi: 10.1109/ICECS.2007.4510929.
- [15] Radiation coupling of a disk to a plane and back or a disk to a disk: An exact solution, Rhyne, Theodore L., The Journal of the Acoustical Society of America, 61, 318-324 (1977).
- [16] Beigelbeck R., Antlinger H., Cerimovic S., Clara S., Keplinger F., Jakoby B.: Resonant pressure wave setup for simultaneous sensing of longitudinal viscosity and sound velocity of liquids, in: Measurement Science and Technology, Volume 24, Number 12, Page(s) 125101, 2013.
- [17] T. A. Litovitz and C. M. Davis, "Structural and shear relaxation in liquids," in Physical Acoustics, vol. II, Part A, W. P. Mason, Ed. New York: Academic Press, 1965, pp. 281–349.